

Proceedings

# Cu.BTC MOF as a Novel and Efficient Catalyst for the Synthesis of 1,8-Dioxo-octa-hydro Xanthene †

Hossein Ghafuri \*, Fatemeh Ganjali and Peyman Hanifehnejad

Catalysts and Organic Synthesis Research Laboratory, Department of Chemistry, Iran University of Science and Technology, Tehran 16846-13114, Iran; fatemeh\_ganjali@chem.iust.ac.ir (F.G.);

p\_hanifehnejad@chem.iust.ac.ir (P.H.)

\* Correspondence: ghafuri@iust.ac.ir

† Presented at the 24th International Electronic Conference on Synthetic Organic Chemistry, 15 November–15 December 2020; Available online: <https://ecsoc-24.sciforum.net/>.

Published: date

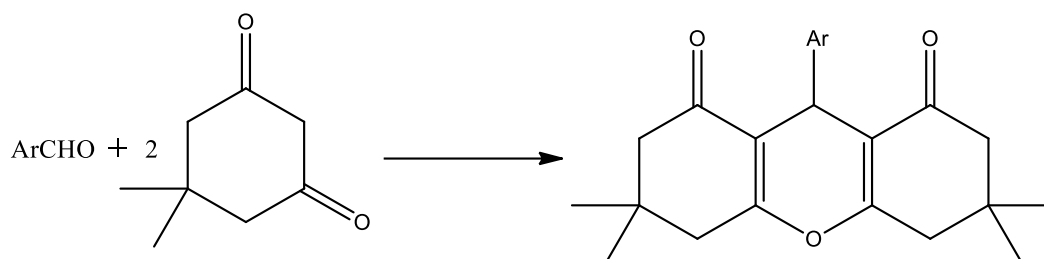
**Abstract:** A copper-based metal-organic framework with 1,3,5-tricarboxylic acid linkers was prepared through a facile hydrothermal method. This MOF has not been used in organic reactions widely. Cu.BTC was employed as an affordable, competent heterogeneous catalyst in 1,8-dioxo-octa-hydro xanthene synthesis. Additionally, the structure, morphology, and porosity of this catalyst were considered. Various techniques such as FE-SEM, BET, EDS, FT-IR, and XRD applied to this aim. As a result, Cu.BTC had a mesoporous structure, an excellent specific surface area, and high purity. Some privileges of using this heterogeneous catalyst in 1,8-dioxo-octa-hydro xanthene synthesis are mild condition, increased activity, ease in separation, and reusability. Also, 1,8-dioxo-octa-hydro xanthene was obtained via simple recrystallization.

**Keywords:** Cu.BTC MOF; catalyst; 1,8-dioxo-octa-hydro xanthene synthesis; xanthene

## 1. Introduction

Multicomponent reactions (MCR) are a synthetic methodology that involves three or more components to produce products having all initiating materials in their structure and almost no by-products [1]. Heterocyclic compounds are one of the condensation MCR products. Additionally, heterocyclic compounds have various photodynamic therapy applications as sensitizers and dyes [2]. Xanthene derivatives are compounds that are obtained from condensation reactions. Xanthene has received recognition as a significant class of organic compounds. According to their bright spectroscopic properties, xanthene compounds are used as dyes and laser technologies. There are other noticeable pharmaceutical and biological properties of xanthene compounds such as anti-viral, antibacterial, antinociceptive, and anti-inflammatory activities [3]. Xanthene compounds are the product produced in two- or three-component reaction aided by a homogeneous or a heterogeneous catalyst. Any material that increases the rate of a chemical reaction without consumption is a catalyst. Xanthene derivatives synthesis various protocols have been upgraded due to organic and medical research scopes in recent years. Several catalysts have been applied in condensation reactions including TiCl<sub>4</sub> [12], amine-functionalized montmorillonite, MOFs [4]. The mentioned catalytic routes have provided important successes; however, some of them bring limitations like low yields, long reaction times, excess of organic solvent, high temperatures, and harsh reaction conditions. MOFs are 3D framework structures with metal centers and organic ligands, widely used as heterogeneous catalysts in many chemical reactions [15]. It is proved that not only the metal clusters of MOFs but their organic ligands have catalytic activity. Moreover, the guest molecules in MOFs can act as catalysts in the same way. One of the well-known copper metal-organic frameworks (Cu.BTC) displays high catalytic activity regarding its unsaturated open copper metal sites [5].

In this literature, Cu.BTC was synthesized through a solvothermal method. As demonstrated in Scheme 1, this catalyst was applied in 1,8-dioxo-octa-hydro xanthene synthesis. High yields, short reaction time, use of non-toxic solvents, and mild reaction condition are the advantage of using this catalyst.



**Scheme 1.** Synthesis of 1,8-dioxo-octahydroxanthenes catalyzed by CU.BTC.

## 2. Experimental

### 2.1. Materials

The Merck Company provided all the chemicals and solvents used for this research and used as received without any further purification.

### 2.2. Synthesis of Cu.BTC MOF

First of all, 1.56 mmol  $\text{Cu}(\text{NO}_3)_2 \cdot 3\text{H}_2\text{O}$  was dissolved in 3 mL distilled water in a beaker, and 0.5 mmol  $\text{H}_3\text{BTC}$  was dissolved in 3 mL ethanol in another beaker simultaneously. Then, two solutions were mixed and stirred for 20 min to obtain a homogeneous mixture. It is sealed in a 60 mL Teflon-lined autoclave and heated at 120 °C for 12 h. In the end, the blue crystals were washed with distilled water and ethanol several times and dried at 60 °C in an oven for 8 h.

### 2.3. Synthesis of 1,8-Dioxo-octa-hydro Xanthene Derivatives

1.0 mmol aldehyde, 2.0 mmol dimedone, 20 mg Cu.BTC and 3 mL ethanol as a solvent were mixed and refluxed for the appropriate time. After completing the reaction (monitored by TLC), the catalyst has filtered, and the solvent evaporated by vacuum. Simple recrystallization has obtained the intended product.

## 3. Characterization

TESCAN, MIRA III detector SAMX field emission scanning electron microscope (FE-SEM) exhibited the sample's morphology. Powder X-ray diffraction (XRD) patterns of the samples were presented by PHILIPS-PW 1800 diffractometer with monochromatized  $\text{Cu K}\alpha$  radiation ( $\lambda = 1.542 \text{ \AA}$ ). FT-IR studies were recorded on a Shimadzu- FT-IR 8400S Spectrometer using KBr pellets at room temperature. TESCAN, MIRA III detector SAMX Energy-dispersive X-ray spectroscopy (EDS) showed qualitative and quantitative elemental analysis and the sample's chemical characterization. Micrometrics ASAP 2020 Brunauer–Emmett–Teller (BET) proved the measurement of the sample's specific surface area. The observations were very often referred to as physical adsorption or physisorption. Thin layer chromatography (TLC) was used for the purity determination of substrates, products and reaction monitoring over silica gel 60 F254 aluminum sheet. Melting points were measured in open capillary tubes with Electrothermal 9100 melting point apparatus.

## 4. Results and Discussion

### 4.1. FE-SEM

The scanning electron microscope (SEM) images of Cu.BTC are presented in Figure 1a,b from two different sides and magnifications 2  $\mu\text{m}$  and 200 nm, respectively. Figure 1a indicates a well crystalline morphology of the Cu.BTC seeds and a very uniform distribution [6]. Figure 1b shows the metal-organic framework from a very close side to show the porous structure [6].

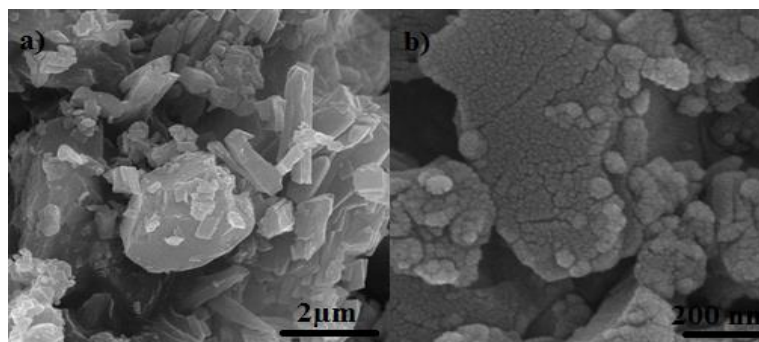


**Figure 1.** SEM images of CU.BTC in different sides and magnifications (a) 2  $\mu\text{m}$  and (b) 200 nm.

### 4.2. XRD

The crystalline structure and phase purity of as-prepared Cu.BTC is determined by XRD pattern. Figure 2 displayed the structure of Cu.BTC matches with ICDD pdf number 00-062-1183 reference card. The diffraction peaks at  $2\theta$  values of 6.7, 10.36, 11.64, 13.48, 14.7, 19.28, 25.92, and 28.92 are attributed to the reflection of planes with (2 0 0), (2 2 0), (2 2 2), (4 0 0), (3 3 1), (4 4 0), (7 3 1), and (7 5 1) miller indices, respectively [7].

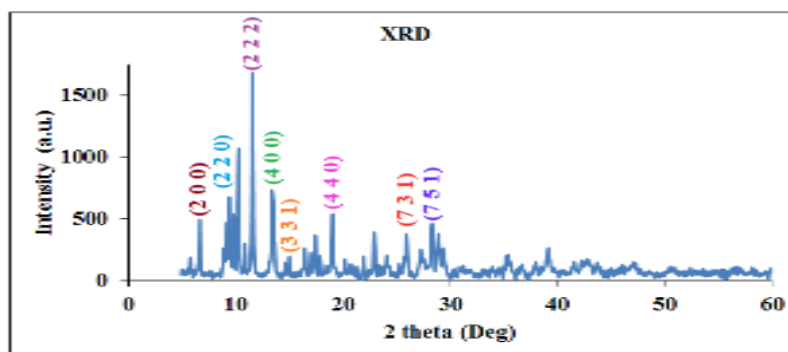


**Figure 2.** XRD pattern of CU.BTC.

### 4.3. EDS

Energy-dispersive X-ray spectroscopy (EDS) confirmed the elements that existed in Cu.BTC and chemical composition of Cu.BTC. Figure 3 shows the original peaks of the sample elements and Figure 4 approved that [8]. The elements originated from Cu  $(\text{NO}_3)_2 \cdot 3\text{H}_2\text{O}$  metal cores and  $\text{H}_3\text{BTC}$  as organic linkers [8].

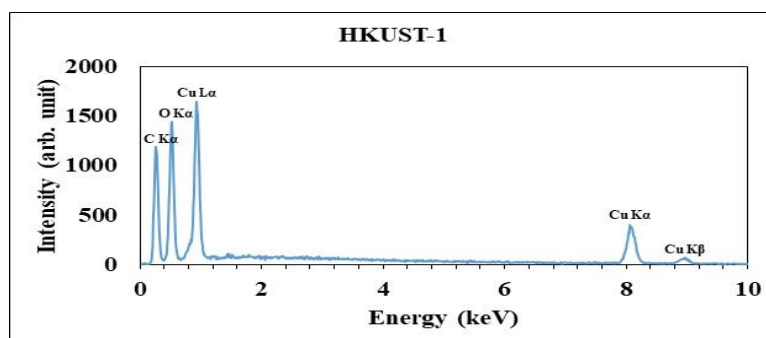


Figure 3. Original peaks of the sample elements.

#### Quantitative Results

Elt	Line	Int	Error	K	Kr	W%	A%	ZAF	Formula	Ox%	Pk/Bg	Class	LConf	HConf	Cat#
C	Ka	835.4	51.5980	0.5263	0.1860	46.13	57.27	0.4032		0.00	81.02	A	45.13	47.14	0.00
O	Ka	906.8	132.3060	0.2417	0.0854	43.14	40.21	0.1980		0.00	72.26	A	42.24	44.04	0.00
Cu	Ka	597.0	0.8812	0.2320	0.0820	10.73	2.52	0.7639		0.00	31.67	A	10.46	11.01	0.00
				1.0000	0.3534	100.00	100.00			0.00					0.00

Figure 4. Quantitative results of Cu.BTC.

#### 4.4. FT-IR

FT-IR spectrum of Cu.BTC is shown in Figure 5. The broad bands at 3000–3500  $\text{cm}^{-1}$  are attributed to stretching vibrations of hydroxyl groups. The three observed peaks at 1437, 1579, and 1623  $\text{cm}^{-1}$  are ascribed to asymmetric, and symmetric carboxylate groups existed in 1,3,5-benzene tricarboxylic acid, respectively. The occurrence of the peak at 1100  $\text{cm}^{-1}$  is related to stretching vibrations of C-O bonds. The peak at 490  $\text{cm}^{-1}$  is assigned to M (Cu)-O bonds [9].

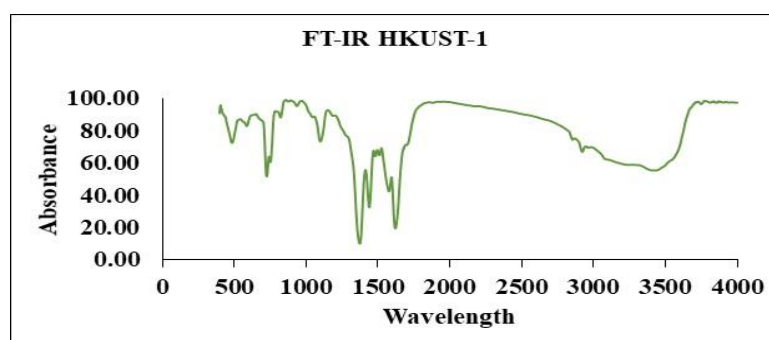
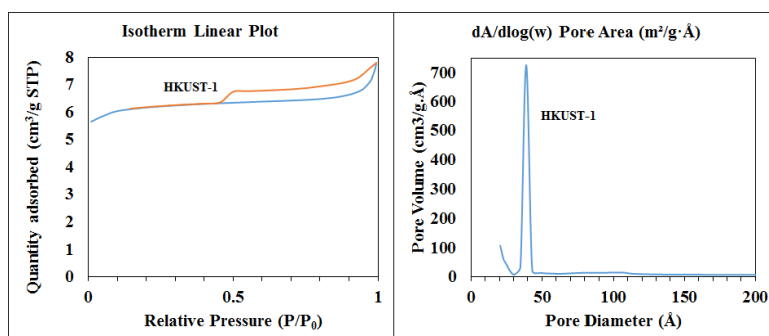


Figure 5. FT-IR spectrum of CU.BTC.

#### 4.5. BET

Brunauer–Emmett–Teller (BET) proved the meso- and micro-porous structure of Cu.BTC with a pore diameter of about 40 Å. The pores' size distribution and pores volume shown in Figure 6 confirmed the MOF structure's mesoporosity [10].

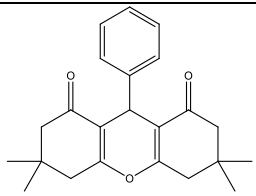
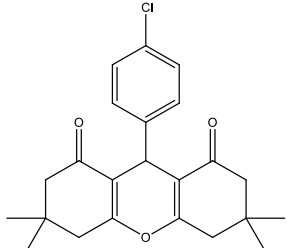
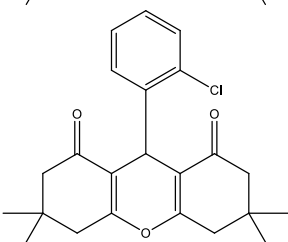


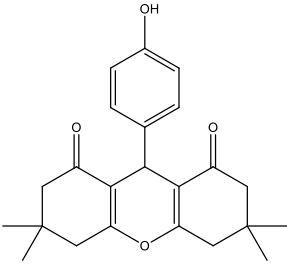
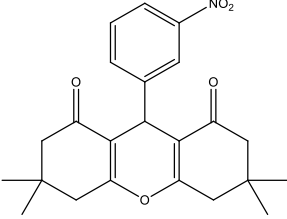
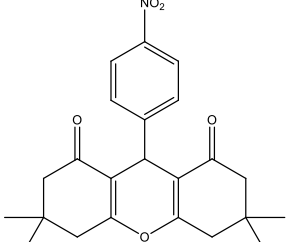
Moreover, BET and Langmuir surface area, the cumulative volume of pores, and the average pore width of the sample are presented in Table 1 that exhibit a high surface area of the MOF.

**Table 1.** BET and Langmuir surface area.

Sample	BET Surface Area m²/g	Langmuir Surface Area m²/g	BJH Desorption Cumulative Volume of Pores cm³/g	BJH Desorption Average Pore width Å
HKUST-1	463.3874	613.5577	0.080150	60.639

To indicate the merits of Cu.BTC in organic synthesis, we have applied that in the synthesis of 1,8-Dioxo-octa-hydro xanthene Derivatives. The reaction didn't conclude without the Cu.BTC and this shows the importance of the catalyst. In Table 2, the aldehyde derivatives used have been reported, and all the products have high yields.

Entry	Product	Time (min)	Yield (%)	Mp °C (Ref.)
1		15	92	201–203 [11]
2		12	88	230–232 [11]
3		18	90	227–229 [11]

4		15	86	246–248 [11]
5		20	89	169–170 [11]
6		20	89	220–222 [11]

## 5. Conclusions

In this study, an excellent catalytic activity of Cu.BTC has investigated. The structure, morphology, and catalytic activity of the MOF have been studied. The Cu.BTC exhibited good porosity and high purity, which are following BET and XRD, respectively, and were synthesized by a facile hydrothermal method.

The results of this research showed Cu.BTC is an efficient heterogeneous catalyst in synthesizing 1,8-Dioxo-octa-hydro xanthene Derivatives in a one-pot multicomponent reaction. This method's benefits are high yields, short reaction time, use of non-toxic solvents, simple workup by recrystallization, and mild reaction conditions. This MOF also could be used as an absorbent for pollutant elimination aims.

**Acknowledgments:** The authors gratefully acknowledge the partial support by Iran University of Science and Technology.

## Reference

- Ganem, B. Strategies for innovation in multicomponent reaction design. *Acc. Chem. Res.* **2009**, *42*, 463–472.
- Evdokimov, N.M.; Kireev, A.S.; Yakovenko, A.A.; Antipin, M.Y.; Magedov, I.V.; Kornienko, A. One-step synthesis of heterocyclic privileged medicinal scaffolds by a multicomponent reaction of malononitrile with aldehydes and thiols. *J. Org. Chem.* **2007**, *72*, 3443–3453.
- Nile, S.H.; Khobragade, C.N. In vitro anti-inflammatory and xanthine oxidase inhibitory activity of *Tephrosia purpurea* shoot extract. *Nat. Prod. Commun.* **2011**, *6*, 1934578X1100601006.
- Parmar, B.; Patel, P.; Murali, V.; Rachuri, Y.; Kureshy, R.I.; Noor-ul, H.K.; Suresh, E. Efficient heterogeneous catalysis by dual ligand Zn (II)/Cd (II) MOFs for the Knoevenagel condensation reaction: Adaptable synthetic routes, characterization, crystal structures and luminescence studies. *Inorg. Chem. Front.* **2018**, *5*, 2630–2640.
- Nobar, S.N. Cu-BTC synthesis, characterization and preparation for adsorption studies. *Mater. Chem. Phys.* **2018**, *213*, 343–351.
- Mao, Y.; Cao, W.; Li, J.; Liu, Y.; Ying, Y.; Sun, L.; Peng, X. Enhanced gas separation through well-intergrown MOF membranes: Seed morphology and crystal growth effects. *J. Mater. Chem. A* **2013**, *1*, 11711–11716.
- Chen, Y.; Mu, X.; Lester, E.; Wu, T. High efficiency synthesis of HKUST-1 under mild conditions with high BET surface area and CO<sub>2</sub> uptake capacity. *Prog. Nat. Sci. Mater. Int.* **2018**, *28*, 584–589.

8. Lestari, W.W.; Ni'maturrohmah, D.; Arrozi, U.S.F.; Suwarno, H. Mg 2+ Doped into Electro-synthesized HKUST-1 and Their Initial Hydrogen Sorption Properties. *Mater. Sci. Eng.* **2018**, *299*, 012031.
9. Azad, F.N.; Ghaedi, M.; Dashtian, K.; Hajati, S.; Pezeshkpour, V. Ultrasonically assisted hydrothermal synthesis of activated carbon–HKUST-1-MOF hybrid for efficient simultaneous ultrasound-assisted removal of ternary organic dyes and antibacterial investigation: Taguchi optimization. *Ultrason. Sonochem.* **2016**, *31*, 383–393.
10. Duan, C.; Li, F.; Li, L.; Zhang, H.; Wang, X.; Xiao, J.; Xi, H. Hierarchically structured metal–organic frameworks assembled by hydroxy double salt–template synergy with high space–time yields. *CrystEngComm* **2018**, *20*, 1057–1064.
11. Nasreen, A. Cupric Nitrate Catalyzed Efficient and Facile Synthesis of 1,8-Dioxo-octahydroxanthene Derivatives. *Asian J. Chem.* **2013**, *25*, 7535–7538.

**Publisher's Note:** MDPI stays neutral with regard to jurisdictional claims in published maps and institutional affiliations.



© 2020 by the authors. Submitted for possible open access publication under the terms and conditions of the Creative Commons Attribution (CC BY) license (<http://creativecommons.org/licenses/by/4.0/>).